

From Field to Museum Studies from Melanesia in Honour of Robin Torrence

edited by

Jim Specht, Val Attenbrow, and Jim Allen

Specht, Jim, Val Attenbrow, and Jim Allen. 2021. Preface	1
Neall, Vincent, Lucy McGee, Michael Turner, Tanya O'Neill, Anke Zernack, and J. Stephen Athens. 2021. Geochemical fingerprinting of Holocene tephra in the Willaumez Isthmus District of West New Britain, Papua New Guinea	5
Pengilley, Alana. 2021. Geochemistry and sources of stone tools in south-west New Britain, Papua New Guinea	25
Shaw, Ben, and Simon Coxe. 2021. Cannibalism and developments to socio-political systems from 540 BP in the Massim Islands of south-east Papua New Guinea	47
Ford, Anne, Vincent Kewibu, and Kenneth Miamba. 2021. Avanata: a possible Late Lapita site on Fergusson Island, Milne Bay Province, Papua New Guinea	61
Hogg, Nicholas W. S., Glenn R. Summerhayes, and Yi-lin Elaine Chen. 2021. Moving on or settling down? Studying the nature of mobility through Lapita pottery from the Anir Islands, Papua New Guinea	71
Lentfer, Carol J., Alison Crowther, and Roger C. Green. 2021. The question of Early Lapita settlements in Remote Oceania and reliance on horticulture revisited: new evidence from plant microfossil studies at Reef/Santa Cruz, south-east Solomon Islands	87
Rath, Pip, and Nina Kononenko. 2021. Negotiating social identity through material practices with stone	107
Dickinson, Paul. 2021. Narrow margins: standardised manufacturing of obsidian stemmed tools as evidence for craft specialisation and social networks in mid-Holocene New Britain	119
Reepmeyer, Christian. 2021. Modelling prehistoric social interaction in the south-western Pacific: a view from the obsidian sources in northern Vanuatu	137
Barton, Huw. 2021. The cylindrical stone adzes of Borneo	149
Davies, Susan M., and Michael Quinnell. 2021. Up close and personal: James Edge- Partington in Australia in 1897	169
Lilje, Erna, and Jude Philp. 2021. The dancing trees: objects, facts and ideas in museums	183
Rhoads, James W. 2021. Papuan Gulf spirit boards and detecting social boundaries: a preliminary investigation	195
Bonshek, Elizabeth. 2021. The Longgu community time capsule: contemporary collecting in Solomon Islands for the Australian Museum	219
Sheppard, Peter J. 2021. <i>Tomoko</i> : raiding canoes of the western Solomon Islands	231
Richards, Rhys, and Peter J. Matthews. 2021. Barkcloth from the Solomon Islands in the George Brown Collection	245

Technical Reports of the Australian Museum Online, no. 34, pp. 1–258

12 May 2021



Geochemical Fingerprinting of Holocene Tephra in the Willaumez Isthmus District of West New Britain, Papua New Guinea

VINCENT NEALL¹ , LUCY MCGEE² , MICHAEL TURNER^{1,3} , TANYA O'NEILL^{1,4} ,
ANKE ZERNACK¹ , AND J. STEPHEN ATHENS⁵ 

¹ School of Agriculture and Environment, Massey University, Palmerston North, New Zealand

² The University of Adelaide, Adelaide SA 5005, Australia

³ 22 Basedow Road, Tanunda SA 5352, Australia

⁴ School of Science, The University of Waikato, Hamilton, New Zealand

⁵ International Archaeological Research Institute Inc.,
2081 Young Street, Honolulu, Hawaii 96826, United States of America

ABSTRACT. Electron microprobe analyses were conducted on volcanic glasses extracted from Holocene tephra marker beds on the Willaumez isthmus in West New Britain, Papua New Guinea. These tephra beds are pivotal in the dating of a wide range of human artefacts and manuports found in the intervening buried soils, extending back over the last 40,000 years. Three major groups can be easily separated: W-K1 and 2; W-K3 and 4; and the Dakataua tephra. Of the remaining post-W-K4 tephra, most show slightly higher FeO and CaO and lower SiO₂ contents than the W-K3 and 4 group, although there is some overlap. The combination of these geochemical data sets with the known stratigraphy and radiocarbon dates has helped resolve tephra correlation where these ashes become thin and less visually diagnostic or where pumice has been resorted and redeposited by the Kulu-Dulagi River.

Introduction

The volcanic alignment of the Willaumez Peninsula extends 60 km northwards from the main west-east axis of the island of New Britain in Papua New Guinea, near the provincial capital of Kimbe. Five km west-northwest of Kimbe, the Peninsula joins the main island by a narrow 18 km-wide strip of lowland hereafter referred to as the Willaumez isthmus (Fig. 1). Within this district, since the 1950s, oil palm plantation development has led to extensive deforestation, and the construction of roads has resulted in the cutting of many exposures into the dominantly tephra cover beds. Between these beds are numerous buried soils (palaeosols) in which abundant artefacts and manuports occur (Torrence *et al.*, 1990). Abundant obsidian flakes

extend back over 40,000 years (Torrence *et al.*, 2004) as do less frequent oven (*mumu*) stones. The district is also renowned for being the site of some of the earliest Lapita pottery in the Pacific (Specht and Torrence, 2007; Torrence *et al.*, 2009). Hence the region has been the centre of much archaeological research, principally conducted by staff of the Australian Museum.

Most of the Holocene human settlement has been disturbed by four plinian eruptions (W-K 1 to W-K 4) from the Witori caldera and one from the Dakataua caldera (McKee *et al.*, 2011), with numerous subsequent sub-plinian and phreatomagmatic events from Witori (Table 1). Machida *et al.* (1996) published the reconnaissance tephrochronology of this sequence and Neall *et al.* (2008) have summarised the volcanological impacts on human settlement.

Keywords: Papua New Guinea; New Britain; Willaumez Peninsula; Holocene tephra; geochemical fingerprinting

Corresponding author: Vincent Neall vandaneall@inspire.net.nz

Received: 19 November 2020 **Accepted:** 30 November 2020 **Published:** 12 May 2021 (online only)

Publisher: The Australian Museum, Sydney, Australia (a statutory authority of, and principally funded by, the NSW State Government)

Citation: Neall, Vincent, Lucy McGee, Michael Turner, Tanya O'Neill, Anke Zernack, and J. Stephen Athens. 2021. Geochemical fingerprinting of Holocene tephra in the Willaumez Isthmus District of West New Britain, Papua New Guinea. In *From Field to Museum—Studies from Melanesia in Honour of Robin Torrence*, ed. Jim Specht, Val Attenbrow, and Jim Allen. *Technical Reports of the Australian Museum Online* 34: 5–24. <https://doi.org/10.3853/j.1835-4211.34.2021.1740>

Copyright: © 2021 Neall, McGee, Turner, O'Neill, Zernack, Athens. This is an open access article licensed under a Creative Commons Attribution 4.0 International License (CC BY 4.0), which permits unrestricted use, distribution, and reproduction in any medium, provided the original authors and source are credited.



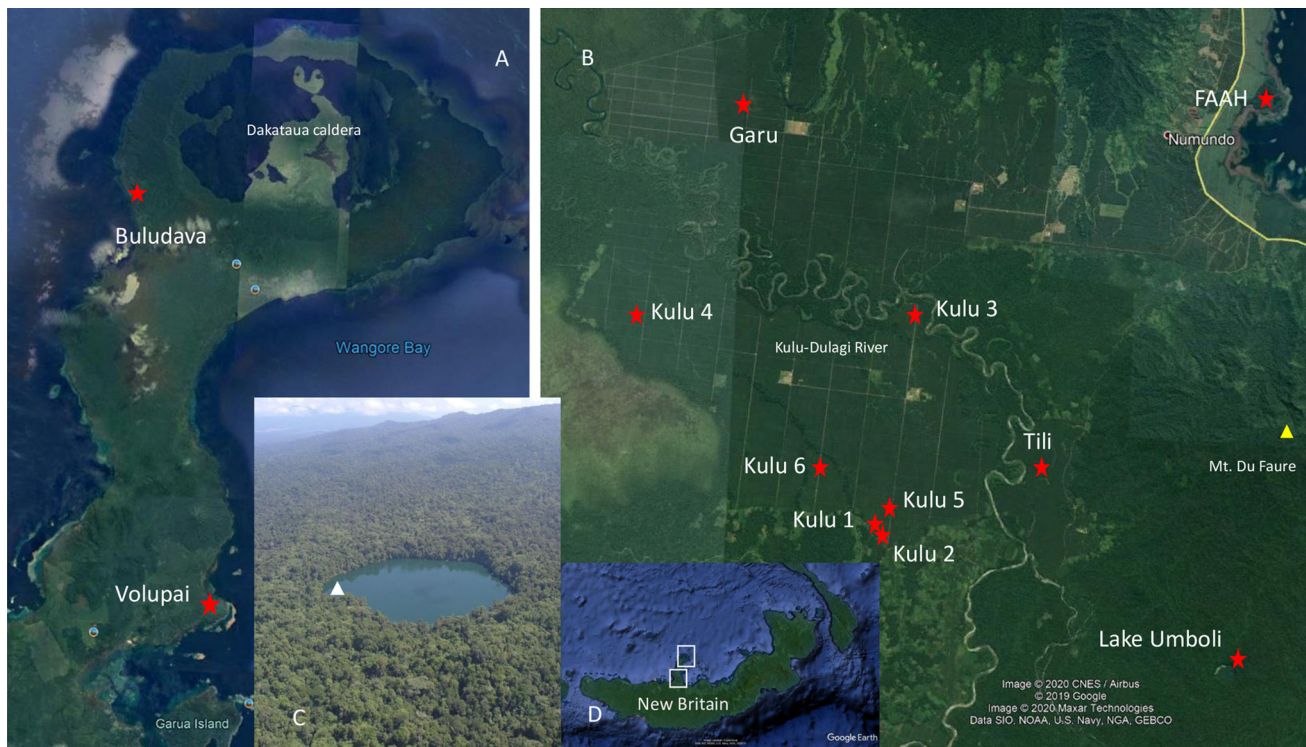


Figure 1. Location of sample sites in this study, West New Britain, Papua New Guinea. (A) northern Willaumez Peninsula; (B) Willaumez isthmus district.; (C) Aerial view of Lake Umboli from the south; white triangle marks location of core site; (D) Map of New Britain showing the Willaumez Peninsula; upper square is area covered by A, and lower square B. Images A, B and C with courtesy of Google Earth.

As the detailed record has emerged, the issue of distinguishing similar appearing plinian and sub-plinian tephra, particularly at distal localities, becomes a problem. In the current study we have applied geochemical fingerprinting of each major Holocene tephra on the

Willaumez isthmus using electron microprobe analysis of volcanic glass. In particular, we have focussed on the post-W-K4 Witori tephra, comprising W-G, H1, H2 and five W-Hs, which are less distinguishable in macroscopic properties from the four major plinian eruptions.

Table 1. Tephra stratigraphy reported by Machida *et al.* (1996) compared with revised chronology used in this paper based on new radiocarbon dates and Petrie and Torrence (2008).

tephra name	Machida <i>et al.</i> , 1996		this paper	
	tephra symbol	age	tephra symbol	age
Witori-Hoskins 7	W-H7	1914 AD?	W-H7	1914 AD ?
Witori-Hoskins 6	W-H6	< 0.5ka	W-H6	post-1426 cal. AD ^a
Witori-Hoskins 5	W-H5	< 0.5 ka	W-H5	1318–1636 cal. AD ^a
Witori-Hoskins 4	W-H4	< 0.5 ka	W-H4	1305–1450 cal. AD ^a
Witori-Hoskins 3	W-H3	0.5 ka	W-H3	1288–1450 cal. AD ^a
Hoskins 2	H2	1.0–0.5 ka	H2	1190–1395 cal. AD ^a
Hoskins 1	H1	1.0–0.5 ka	H1	783–993 cal. AD ^a
Dakataua tephra	Dk	1.15 ka	—	—
Witori-Galilo	W-G	1.2 ka	W-G	783–993 AD ^a
Witori-Kimbe 4	W-K4	1.3–1.5 ka	W-K4	1280 cal. BP ^b
	—	—	Dk	1300 cal. BP ^b
Witori-Kimbe 3	W-K2	1.8 ka	W-K3	1615 cal. BP ^b
Witori-Kimbe 2	W-K2	3.3 ka	W-K2	3315 cal. BP ^b
Witori-Kimbe 1	W-K1	5.6 ka	W-K1	5920 cal. BP ^b

^a 95% confidence interval calibrated radiocarbon age range.

^b Modal radiocarbon dates from Petrie and Torrence (2008).

Table 2. Specific details of sample sites shown in Fig. 1.

map reference (see Fig. 1)	archaeological reference site	geological reference site	latitude (S)	longitude (E)	altitude (m)
Buludava	—	Buludava village	05°04'46.5"	150°01'37.2"	1
FAAH	FAAH XVII	—	05°29'55.6"	150°05'47.4"	15
Garu	—	Garu peat	05°30'24.2"	149°58'48.3"	10
Kulu 1	—	Kulu-1	05°36'18.9"	150°00'56.7"	18
Kulu 2	FACR XXII	—	05°36'20.5"	150°00'58.9"	20
Kulu 3	—	Kulu-13	05°33'21.6"	150°01'17.2"	12
Kulu 4	—	Kulu-14	05°33'25.0"	149°57'28.6"	6
Kulu 5	350 m N of FACQ LXVII	Kulu-15	05°35'54.5"	150°01'04.7"	19
Kulu 6	—	Kulu-10	05°35'22.9"	150°00'02.2"	17
Lake Umboli	—	Lake Umboli-2004	05°38'05.4"	150°05'44.8"	230
Tili	—	Tili-3	05°35'46.8"	150°02'56.6"	20
Volupai	—	Pangalu Estate	05°14'42.7"	150°04'02.3"	28

Materials

Glass chemistry can provide a method to discriminate eruption deposits (in this study, all unidentified tephras) from one eruption to those associated with a different eruption from the same or a different volcanic source (Lowe *et al.*, 2017), and has especially proven to be much more successful with rhyolitic eruptions compared to those of andesitic composition. In this study, we obtained glass shard compositional data from tephras preserved at ten sites on the Willaumez isthmus region, plus two samples from reference sites on the Willaumez Peninsula (Fig. 1A,B; see sites 9 and 11 in fig. 2 of McKee *et al.*, 2011).

The first site is an archaeological site on Numundo Plantation (Fig. 1B) referenced FAAH XVII (Table 2). Its significance is that this site displays the complete sequence of four major Holocene plinian eruptions from the Witori (Pago) caldera with intervening buried soils (for further details see fig. 4 in Neall *et al.*, 2008). The site is on a relatively flat-topped hill away from any downslope accumulation processes that might have led to redeposition. Thus, the primary tephra preservation is exquisite and tephra identification of W-K1, W-K2, W-K3 and W-K4 is unequivocal.

The second site is Lake Umboli, a circular 527 m-diameter water-filled depression located in hill country 10.5 km south-west of Kimbe (Fig. 1B, 1C, and Table 2). At an elevation of approximately 230 m, the lake was measured by us to have a maximum water depth of 32.9 m. Two bottom survey transects were conducted showing a broad 'shallow' concave profile suggestive that the lake is a phreatomagmatic maar. Being located away from any cultivation, the lake is surrounded by native forest to the water's edge, minimising any human-induced erosion into the lake. A 3.6 m-long reference core was obtained from a water depth of 6.82 m, 10 m from the south-western shore of the lake. It provides a continuous record of many primary tephras erupted across the Willaumez isthmus in the last 1400 years. Here the tephras were unidentifiable by macroscopic features alone; hence a framework stratigraphy was established (Fig. 2) before geochemical fingerprinting could be applied.

The third site is on Tili Estate (Fig. 1B, Table 2), alongside a former oxbow of the Kulu-Dulagi River system. Here on a levee, floodwaters have entrapped three tephras within river silts and sands over the last 500 years (Fig. 3).

The fourth site is on Garu Estate (Fig. 1B, Table 2) where five tephras are preserved in peat above the water table (Fig. 4). The palynology of samples obtained from the peats was reported by Jago and Boyd (2005) with three of five

tephras being identified as W-K3, W-K4, and W-G. Note that two further thin (1 cm thick), discontinuous tephras were identified in this study, above Tephra 1 in Jago and Boyd (2005).

Six further sites all located on Kulu Estate, to the west of the Kulu-Dulagi River (Fig. 1B, Table 2), were included in this study to clarify tephra identification. Kulu 1 is in a drain immediately north of the hills that border the Kulu Estate to the south. It is in a peaty, colluvial footslope position where all tephras are likely to be preserved but overthickening is identified due to colluvial redeposition. It was selected to try and resolve the latest W-H tephra sequence (Fig. 5).

Kulu 2 is an archaeological site (FACR XXII) on a hill overlooking the Kulu 1 site. It is a well-drained location with a tephra sequence extending down to the W-Ks, but only the W-H sequence was sampled for this study (Fig. 6).

Kulu 3 is on the northern border of Kulu Estate, close to the bridge across the Kulu-Dulagi River. The surrounding landscape is subdued, yet the tephra sequence extends back to pre-W-K3 time, suggesting this is a former hill almost buried by surrounding alluvium. A distinct tephra above W-K4 was sampled from this site for identification (Fig. 7).

Kulu 4 is a site near the western margin of Kulu Estate, 8 km south-east of the western coastline of the Willaumez isthmus. This location was sampled to identify the tephra beneath 0.9 m of alluvially resorted W-K 2 (Fig. 8).

Kulu 5 is from an auger hole cored to 6.4 m depth, 350 m north of archaeological site FACQ LXVII, near the southern margin of Kulu Estate. This sample was obtained to confirm the identity of the prominent pumiceous tephra between 5 and 6 m depth (Fig. 9).

Kulu 6 is another section near the southern margin of Kulu Estate in a drain at a small riser in the Kulu lowland landscape. Here deep incision into the pumice layers was causing severe erosion (with countermeasures in place). Nearly 50 cm of W-K 3 is preserved here, above redeposited W-K2 (Fig. 10). However, the section was sampled in this study for a post-W-K4 tephra identification at 25 cm depth.

Two reference sites were also sampled on the Willaumez Peninsula to obtain the volcanic glass composition of identified eruptives associated with the Dakataua eruption. One was pumice from pyroclastic-flow deposits of the Dakataua eruption, sampled from a coastal exposure at Buludava on the western flanks of the Dakataua caldera (site 11 in fig. 2 of McKee *et al.*, 2011). The second sample was from a site half-way along the Willaumez Peninsula in the Volupai Plantation district near Pangalu village (site 9 in fig. 2 of McKee *et al.*, 2011).

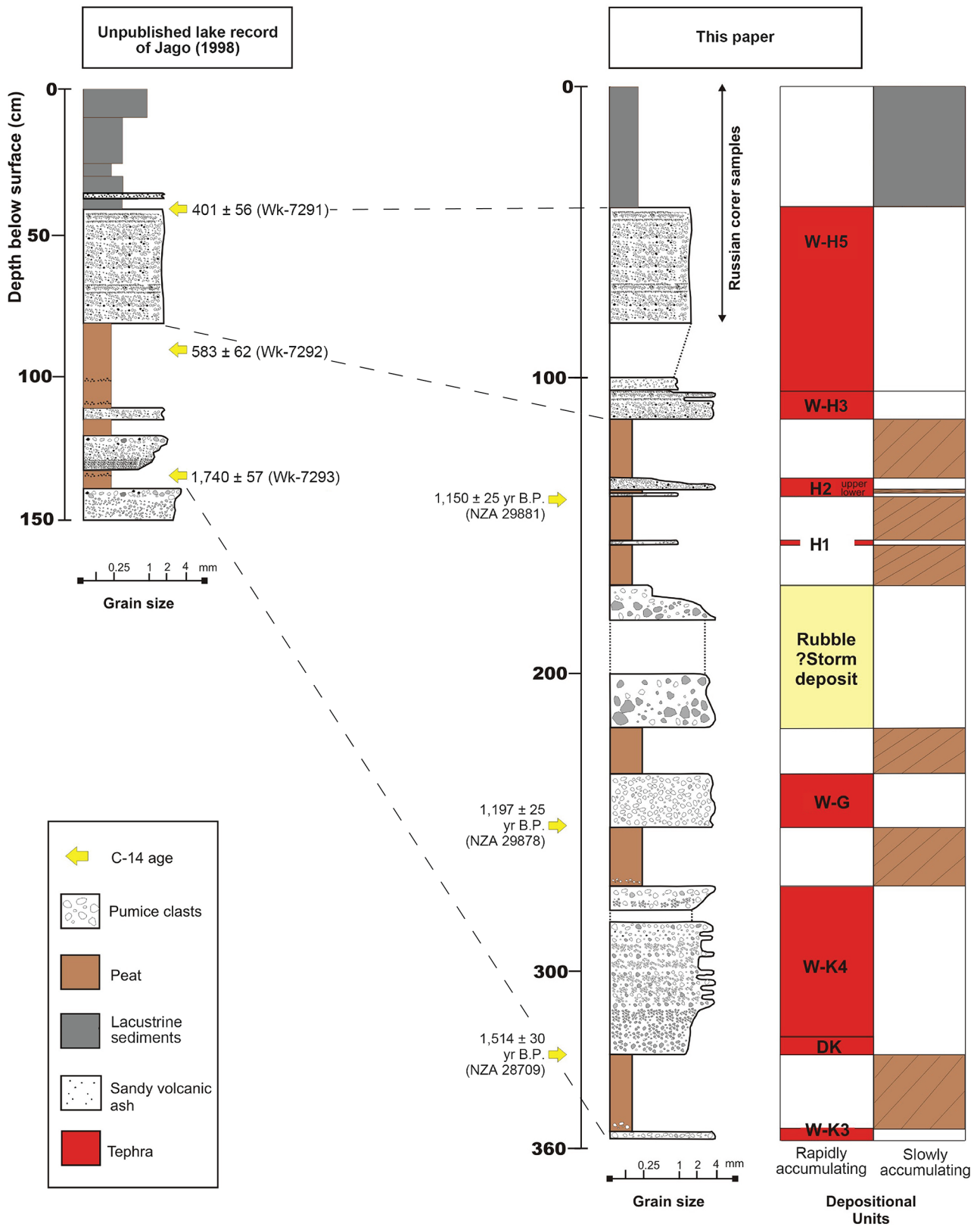


Figure 2. Stratigraphy of core obtained from Lake Umboli, West New Britain. Core beneath 1 m was sampled with a Geo-core piston sampler.

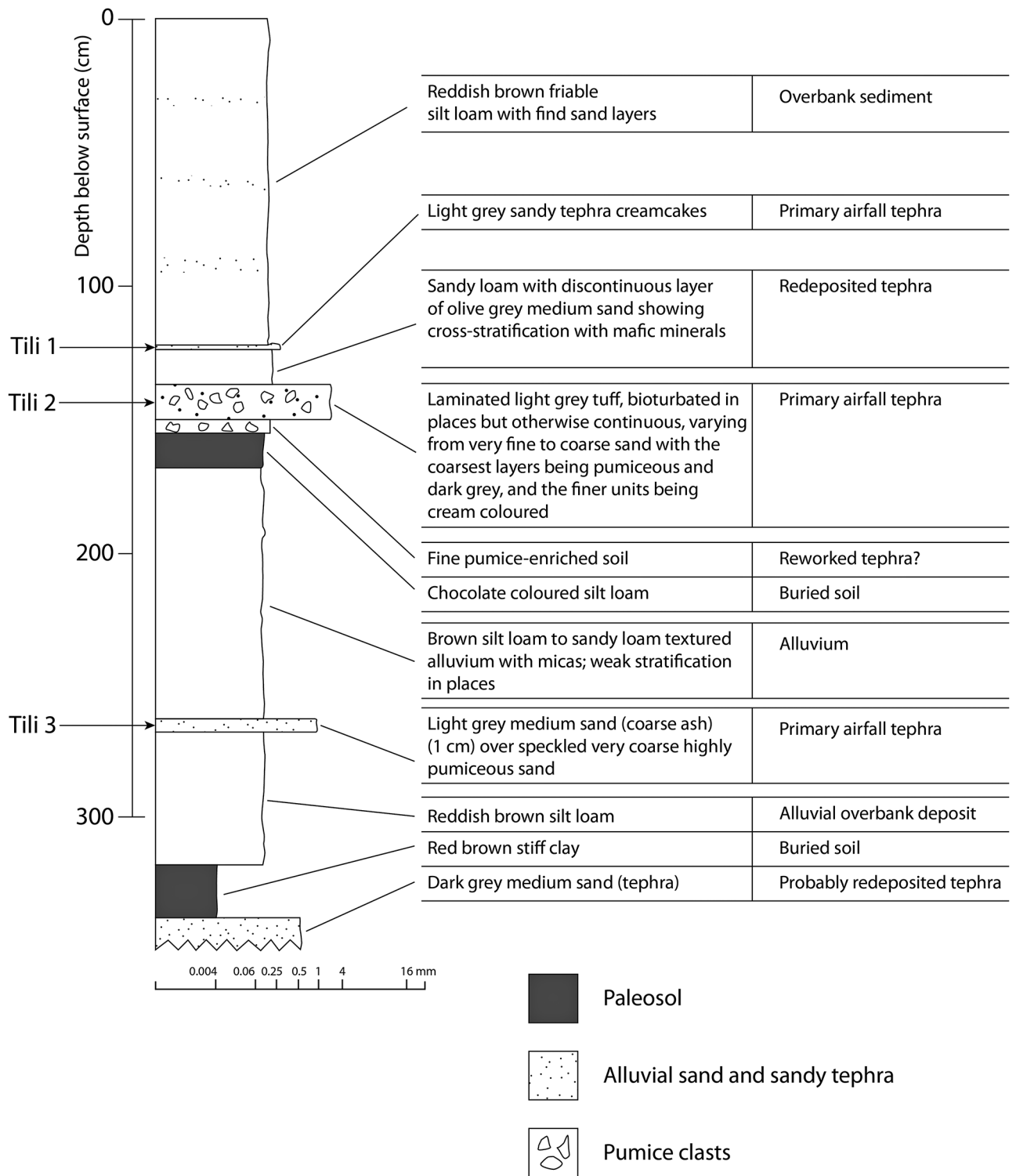


Figure 3. Stratigraphy of Tili site and stratigraphic positions of three tephra samples selected from the W-H sequence.

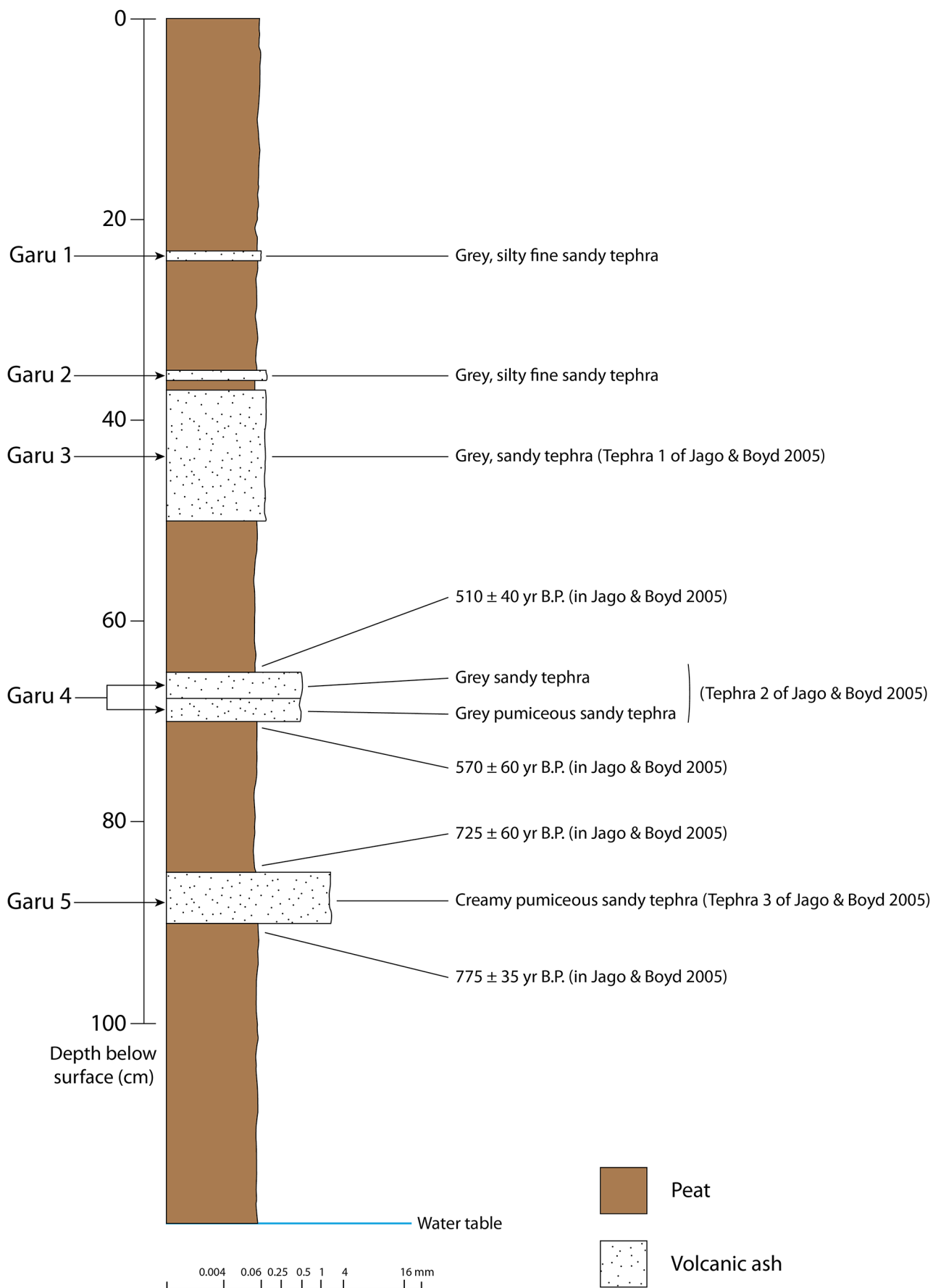


Figure 4. Stratigraphy of Garu site and stratigraphic positions of six tephra samples selected from the post-W-G sequence. Note samples 4 and 5 are from two beds forming a single tephra unit.

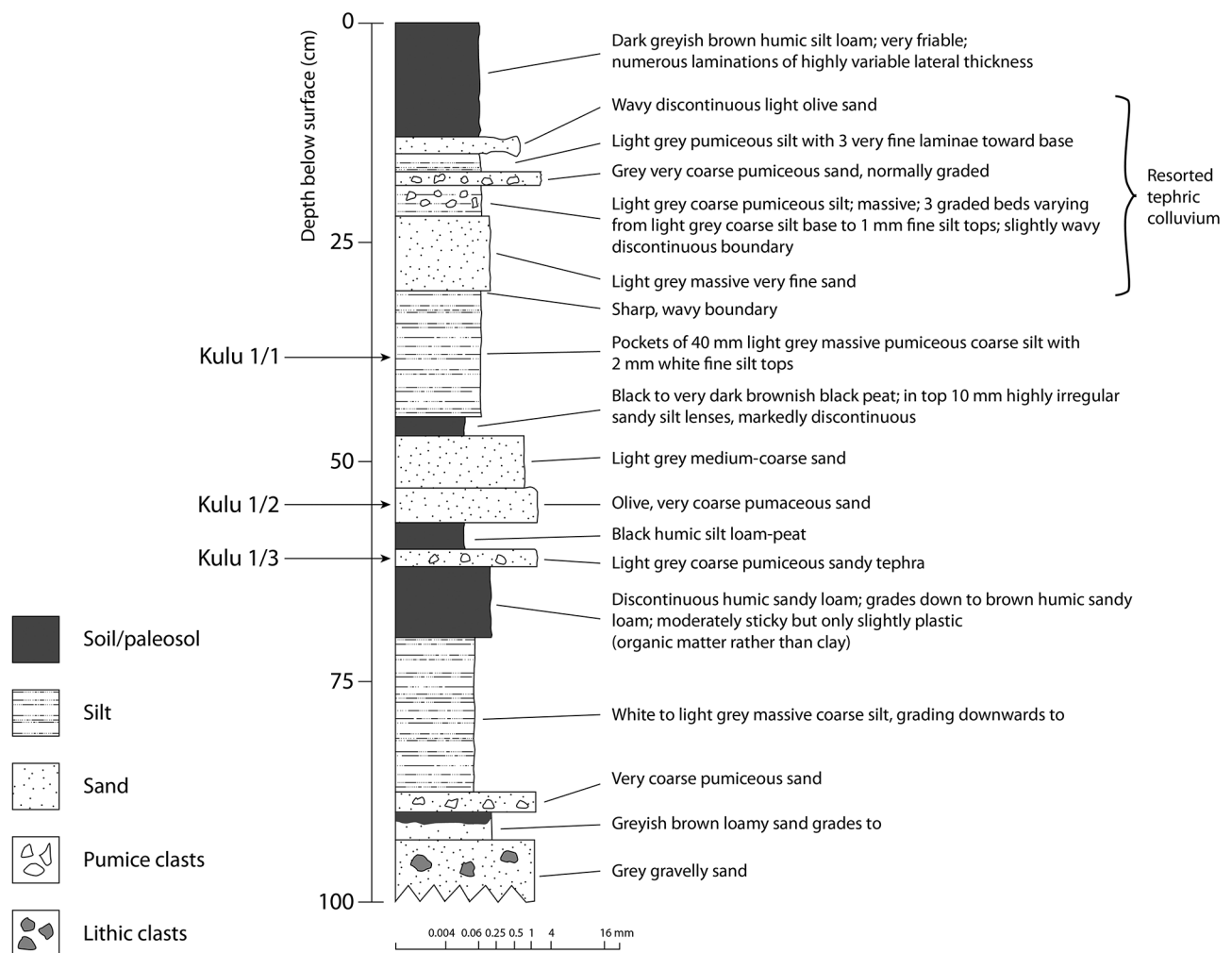


Figure 5. Stratigraphy of Kulu 1 site and stratigraphic positions of three tephra samples selected from the W-H sequence.

Methods

Sampling

The core from Lake Umboli was obtained as follows. First, the softer sediment at the top was sampled with a Russian corer to a depth of 70 cm. It was not possible to retain the loose pumice sand from 70–100 cm depth. Second, the core from 1 m to 3.6 m was obtained with a Geo-core piston sampler recovering sediment and tephra beds into capped aluminium collection tubes. All other samples were from vertical exposures where channel samples were scooped into plastic bags.

Sample preparation

Pumice clasts were washed, carefully crushed with a mortar and pestle, and then sieved. Loose grain samples were just sieved. Glass separates were isolated under a bi-focal microscope from the 125–250 μm fraction. Separates were then mounted in (EpoTek) resin and polished for electron microprobe analysis, using a Struers Planopol-3 and increasingly finer grades of diamond paste (6, 3, and 1 μm).

Electron microprobe

Glass compositions were determined by energy dispersive (EDS) electron microprobe (Jeol JXA-840) at the University of Auckland. The analytical data were collected using a Princeton GammaTech Prism 2000 Si (Li) EDS X-ray detector, a 20 μm de-focused beam accelerating voltage of 12.5 kV, beam current of 600 pA and 100 second live count time. Na_2O was recorded first, due to the volatile nature of Na in the probe beam. Detection limits (1σ in wt%) for this instrument were: SiO_2 0.11, TiO_2 0.08, Al_2O_3 0.06, FeO 0.07, MnO 0.07, MgO 0.07, CaO 0.04, Na_2O 0.11, K_2O 0.03, P_2O_5 0.07, SO_3 0.06, Cl 0.03, Cr_2O_3 0.06, NiO 0.1. An Astimex albite standard was used for calibration at the beginning of each analytical session and show good precision (see Table S1). Elements that were not present in the standard are denoted by italics in Table S1 and are not used in geochemical plots. This microprobe took part (along with 64 other participating laboratories) in the ‘G-Probe-2 international proficiency test for microbeam laboratories’; the results of which were within the acceptable deviation from the NKT-1G basaltic glass standard (e.g., Potts *et al.*, 2005) and within the error of the median values for the standards tested. The deviation from the accepted values for the major elements is listed in Table S1.

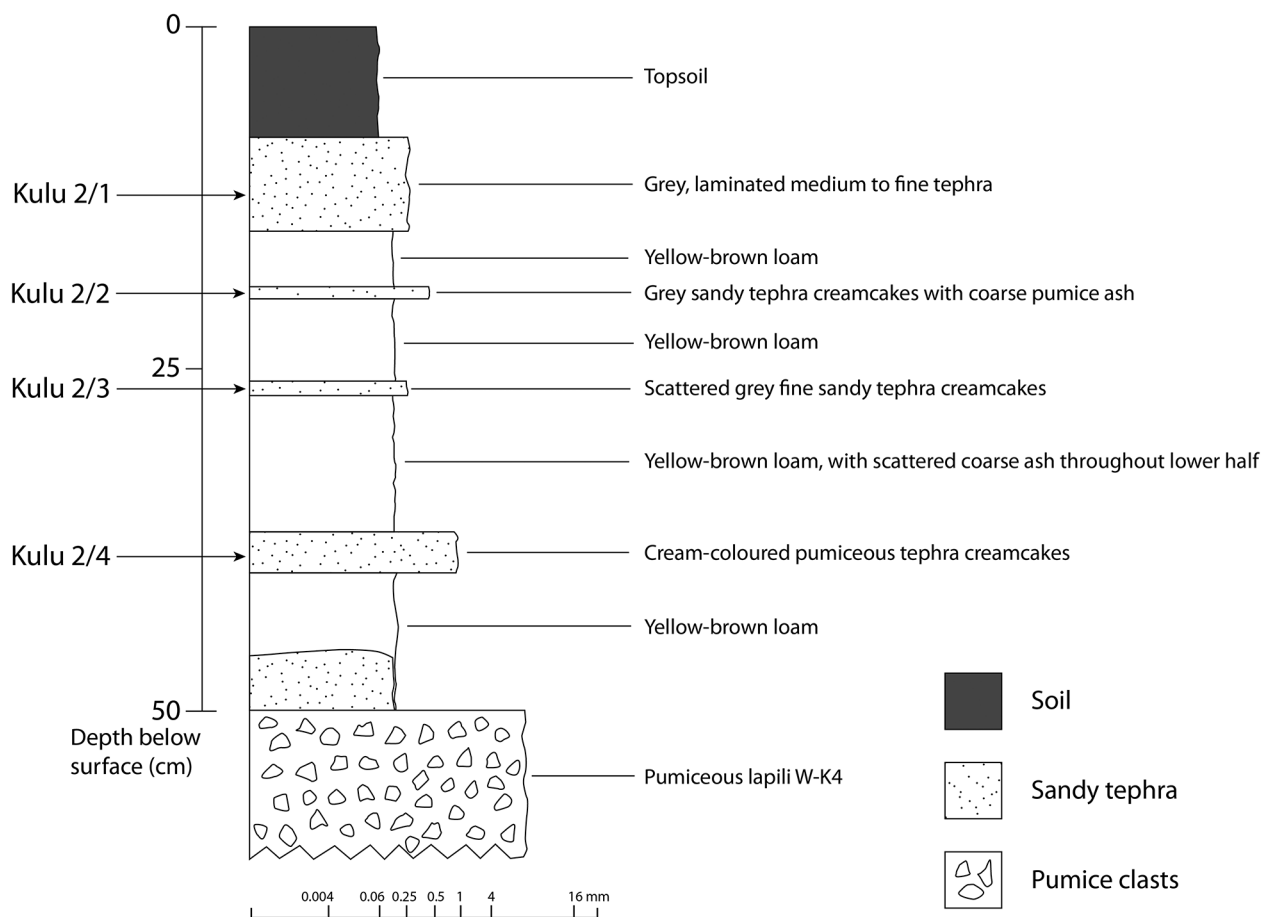


Figure 6. Stratigraphy of Kulu 2 (archaeological site FACR XXII) and stratigraphic positions of four post-W-K4 tephra samples selected.

Tephrochronology

The FAAH locality forms the reference locality for the W-K1 to W-K4 tephras (see Neall *et al.*, 2008).

Three key localities form the basis for the post-W-K4 tephras in the district. The first is the core obtained from Lake Umboli (Fig. 2). Three AMS radiocarbon dates were obtained in this study (NZA 28709, NZA 29878 and NZA 29881). The lowest sample from 329–331 cm depth, immediately below a dark grey coarse ash, was dated on dark brown peaty sediment. The conventional radiocarbon age was 1514±30 BP (NZA 28709; BP = Before Present). This fits with the overlying coarse ash being the Dakataua tephra, which close to source contains charcoal logs within pyroclastic-flow deposits dated at 1370±37 BP (Wk-15505; McKee *et al.*, 2011: table 3). It is notable that in this core there is no sediment preserved between the Dakataua tephra and the overlying W-K4 pumice. This date also demonstrates that the lowest pumice tephra sampled in the core is the W-K3 tephra.

The middle-dated sample was on pollen separated from black fibrous sandy peat at 252–254 cm depth, immediately beneath a prominent pumiceous coarse ash and fine lapilli and yielded a conventional radiocarbon age of 1197±25 BP (NZA 29878). This correlates well with a date of 1190±70 BP (Beta-29257) obtained from above the W-K4 tephra and below the W-G (‘Galilo Pumice’ of Blake, 1976) reported by Machida *et al.* (1996: fig. 4). Hence the pumiceous unit above can be confidently correlated with the Galilo Pumice.

The uppermost dated sample was on a pollen separate from black fibrous silty peat at 140–142 cm depth, immediately beneath a grey pumiceous coarse ash (with

a 1 cm band of black peat within it, clearly separating an earlier and later closely time-spaced event). The resultant conventional radiocarbon age was 1150±25 BP (NZA 29881). Clearly the tephra above is not a W-H tephra based on the evidence that they are all younger than 519±68 BP (NZA 2011) (Machida *et al.*, 1996: fig. 4). Hence, the only likely interpretation is that the tephra above NZA 29881 is Hoskins 2 (H2) of Machida *et al.* (1996), and the tephra 15 cm below it is Hoskins 1 (H1).

Previous unpublished radiocarbon dates obtained by Jago from a compressed core 1.475 m long (obtained from 2.82 m sediment depth) in shallower water (2 m from shore) at Lake Umboli can be directly correlated to this core. These dates (Fig. 2) constrain the youngest tephra sequence in the core to between 401±56 BP (Wk-7291) and 583±62 BP (Wk-7292). This information can be directly correlated to our core described here, demonstrating that the package of tephras between 40 and 114 cm depth in this core represents all or some of the W-H tephras.

The second key locality is located on the Tili oil palm plantation (Fig. 3). Here three post-W-K4 tephras are preserved within overbank silt deposits. No radiocarbon datable material was available at this section, but the clear tephra succession allows a geochemical comparison to be made.

The third key locality is located on the Garu oil palm plantation, 1.1 km west of Boku Hill (Table 1, Fig. 4). Here five tephras have now been identified above peat radiocarbon dated at 775±35 BP (OZF 371) (Jago and Boyd, 2005: table 1). Each was sampled for any distinguishing glass geochemistry of the W-H tephra sequence.

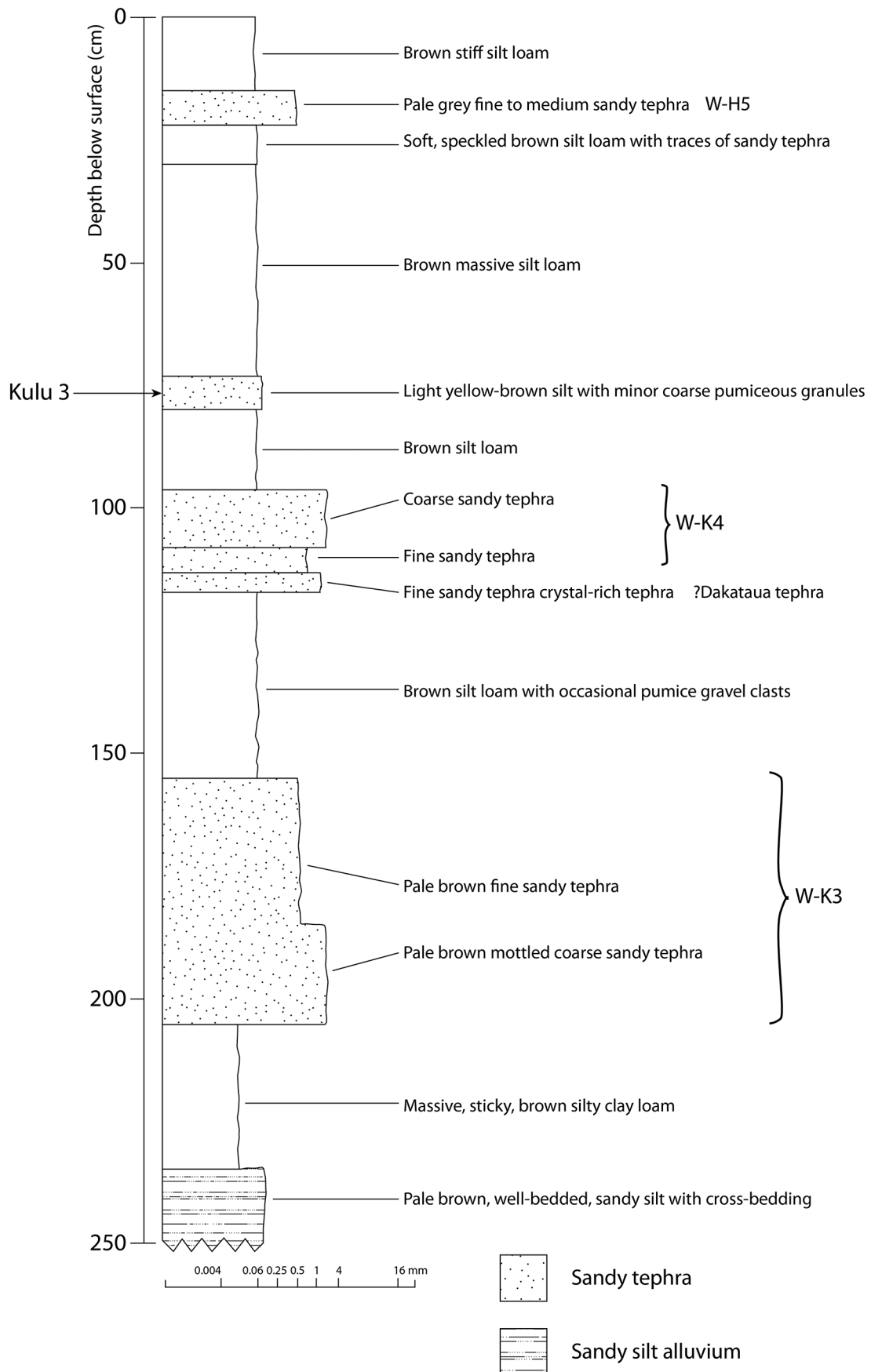


Figure 7. Stratigraphy of Kulu 3 site and stratigraphic position of one post-W-K4 tephra sample selected.

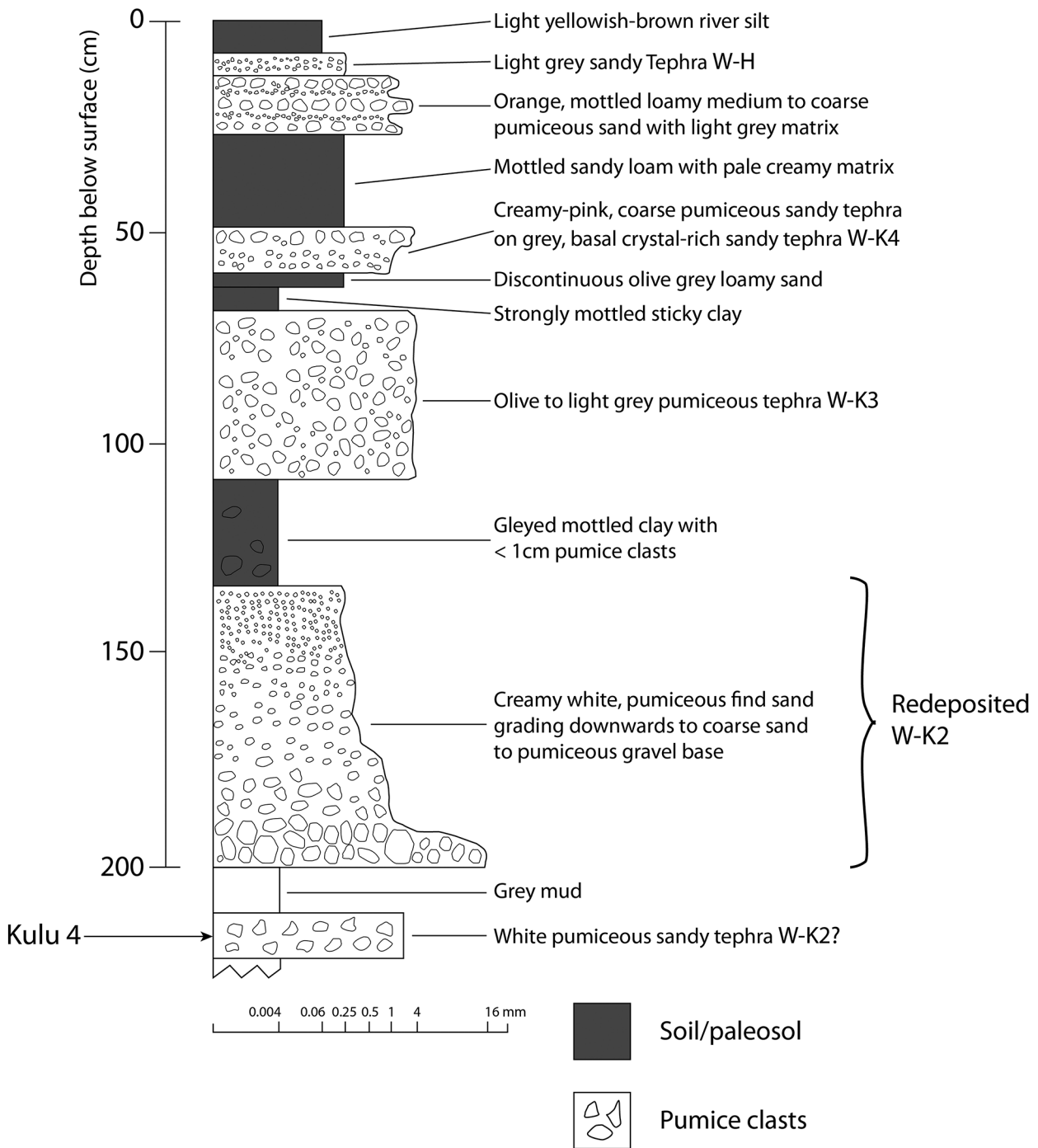


Figure 8. Stratigraphy of Kulu 4 site and stratigraphic position of one pre-W-K3 pumiceous tephra sample selected.

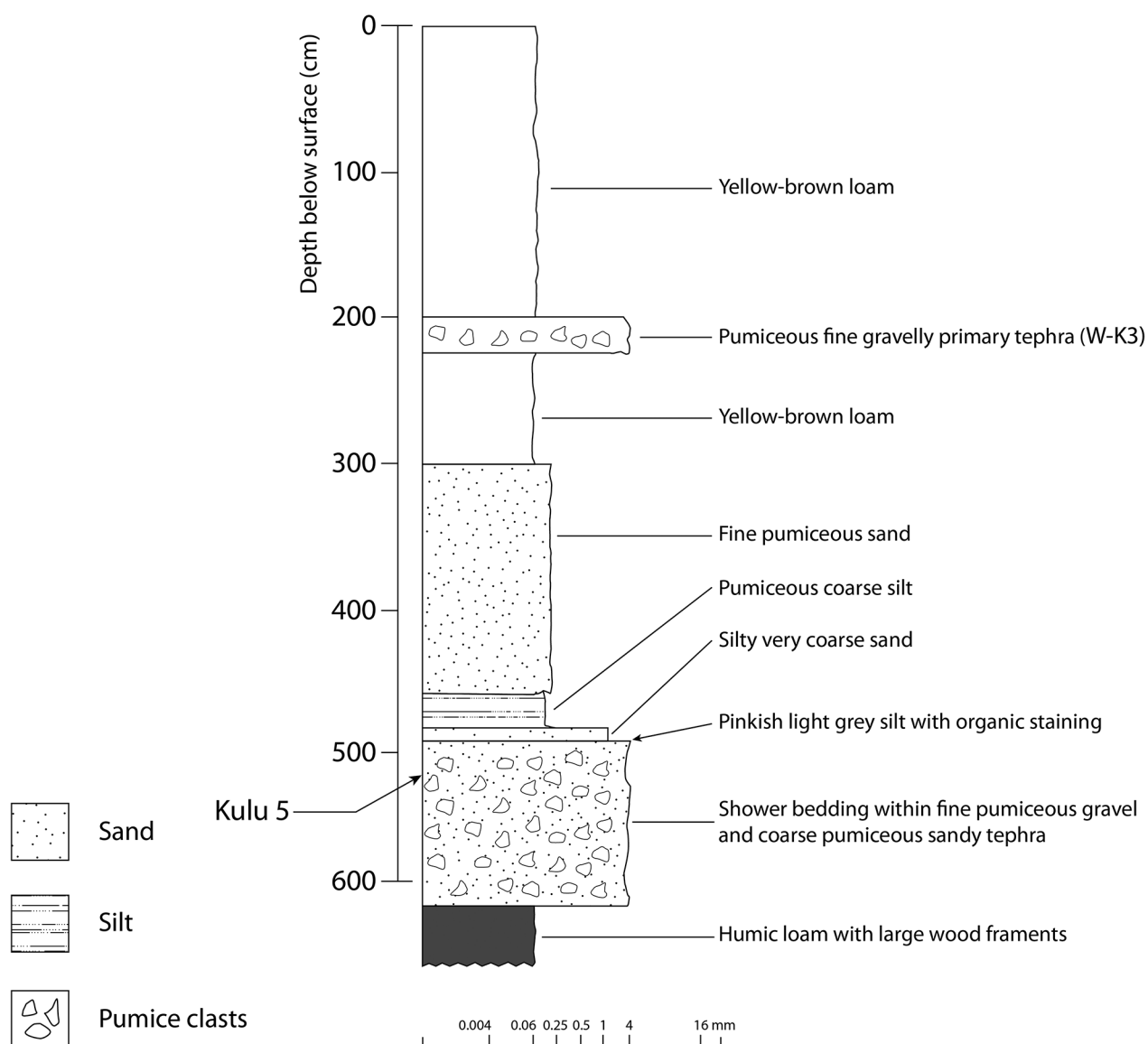


Figure 9. Stratigraphy of Kulu 5 site and stratigraphic position of one pre-W-K3 tephra sample selected from near base of augur hole.

Results

The composition of glass shards between and within the different samples obtained from all sites are presented in Table S1. The figures show data normalised to 100 wt%, and Table S1 presents both raw and normalised data.

Dakataua (DK) tephra from the Buludava and Volupai locations cluster at lower SiO_2 (66.5 wt%) but higher FeO, CaO and Al_2O_3 (5.1, 4.0 and 14.7 wt%, respectively, see Fig. 11) than other tephras in the Willaumez isthmus region, mostly sourced from the Witori caldera. The Dakataua tephra at these locations is identifiable due to the presence of charcoal fragments which are well-dated at 1370 ± 37 BP (Wk-15505) and 1400 ± 43 BP (Wk-11750) (McKee *et al.*, 2011: table 3). Thus, the Dakataua tephra provides a reliable, recognisable marker bed for correlation with other sites in the region.

Tephra layers sampled from the FAAH site fall into two distinctive groups (Fig. 11). First is a high SiO_2 (76–79 wt%), low FeO (1.3–2.3 wt%), low CaO (1.6–1.9 wt%) group consisting of tephras from the plinian W-K1 and W-K2 Witori caldera-sourced eruptions. Second is a group comprising the W-K3 and W-K4 tephras, which have lower SiO_2 (72.5–74.8 wt%, not including outliers) and higher FeO

(2.5–3.8 wt%), CaO (2.9–3.5 wt%) and Al_2O_3 (13.1–13.7 wt%) than the earlier Witori caldera eruptions (W-K1 and W-K2). Samples from Kulu 4 and Kulu 5 correlate to the W-K1 and W-K2 field.

When the geochemistry of tephras encountered in the Lake Umboli core are plotted with respect to the known Dakataua and Witori caldera eruptions (Fig. 12) some can be easily recognised. The lowermost Lake Umboli tephra (at 362–363 cm depth) has the middle SiO_2 -middle FeO signature of the W-K3/4 group tephras. The low SiO_2 -high FeO tephra above this (at 326–329 cm depth) clearly matches the composition of the Dakataua tephra. The tephra at 284–305 cm depth returns to a composition similar to W-K3/4 (although is somewhat bimodal in SiO_2 and CaO content), supporting the proposition that the Dakataua eruption occurred shortly before the W-K4 eruption (McKee *et al.*, 2011) and unequivocally identifying the basal three tephras in the core (Fig. 12).

Trying to geochemically distinguish the post-W-K4 tephras in the Lake Umboli core is difficult due to substantial overlap in geochemical compositions (Fig. 13). However, the Galilo Pumice (W-G) is clearly identified by the radiocarbon date from immediately beneath it (Fig. 2). A further radiocarbon date from immediately beneath

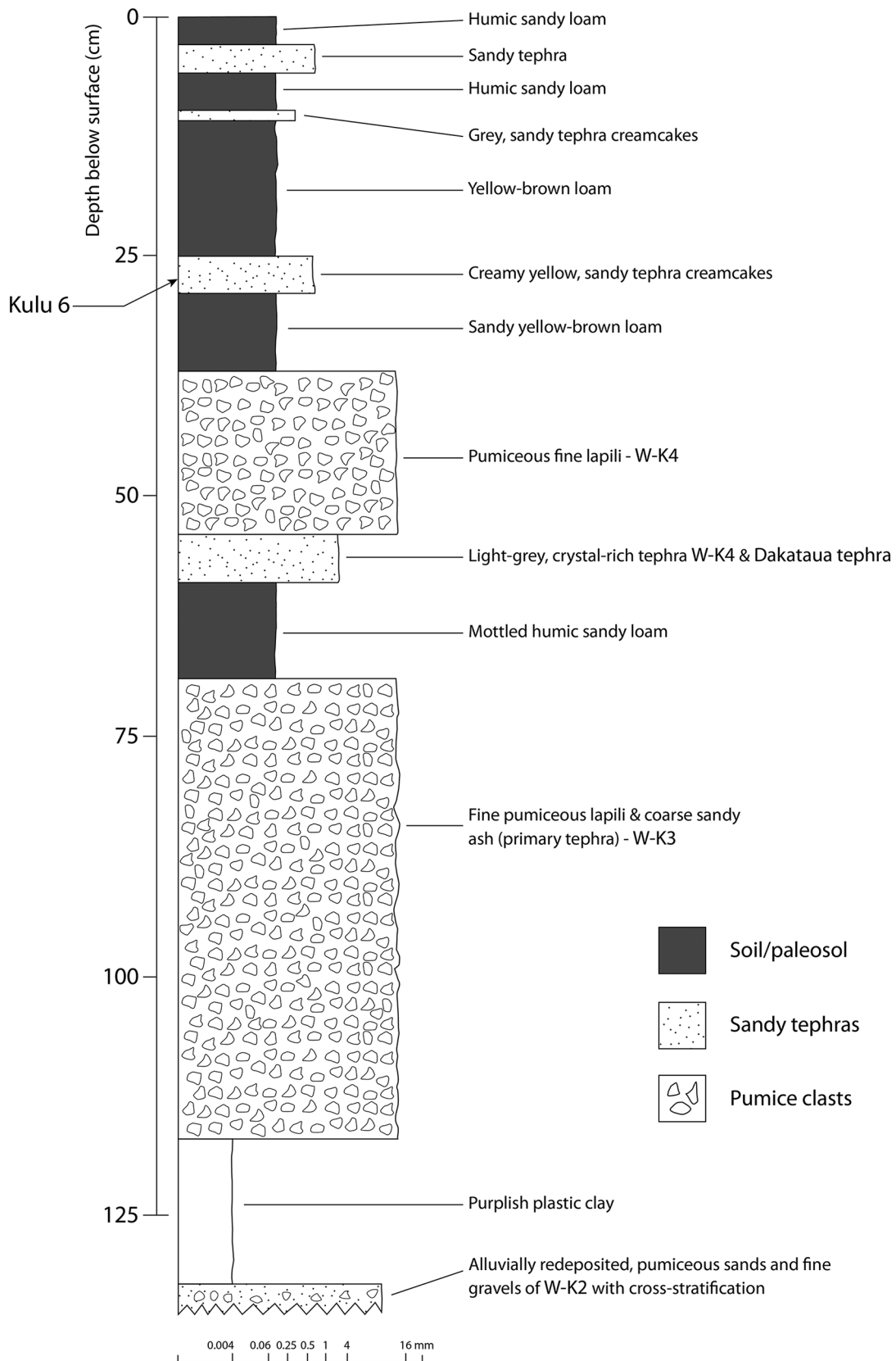


Figure 10. Stratigraphy of Kulu 6 site and stratigraphic position of one post-W-K4 tephra sample selected.

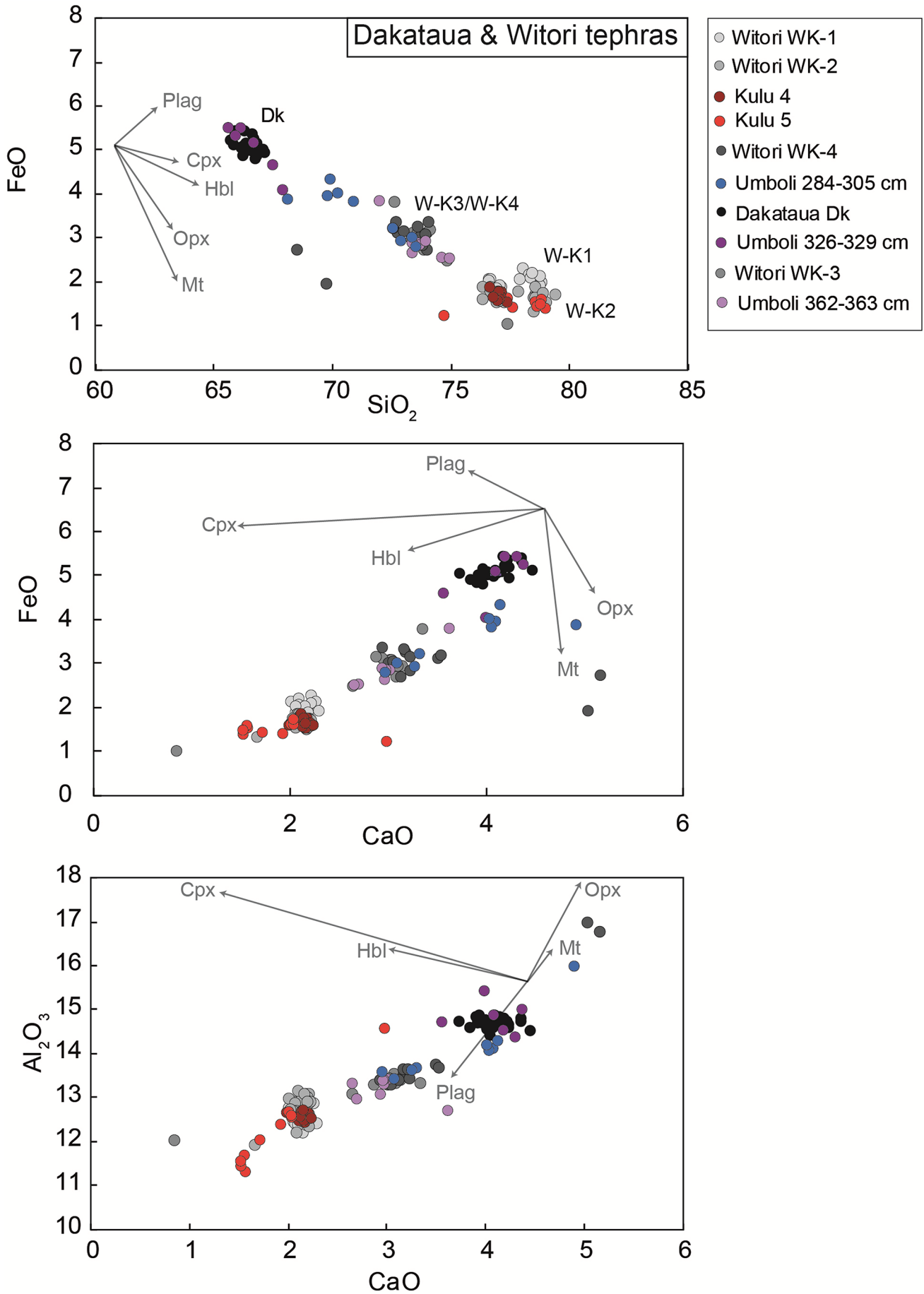


Figure 11. Volcanic glass chemistry for the Dakataua tephra and the four Plinian eruptions from Witori caldera exposed at the FAAH site. Tephras from the Lake Umboli, Kulu 4 and Kulu 5 sites correlate with the W-K1/2, Dakataua and W-K3/4 groups. Vectors portray approximately 15% fractional crystallisation of each mineral, except for magnetite which is approximately 5% crystallisation. Plag = plagioclase, Cpx = clinopyroxene, Hbl = hornblende, Opx = orthopyroxene, Mt = magnetite. Mineral compositions are from the Tauhara dacite in the Taupo Volcanic Zone (Millet *et al.*, 2014); see Table S1 for compositions used.

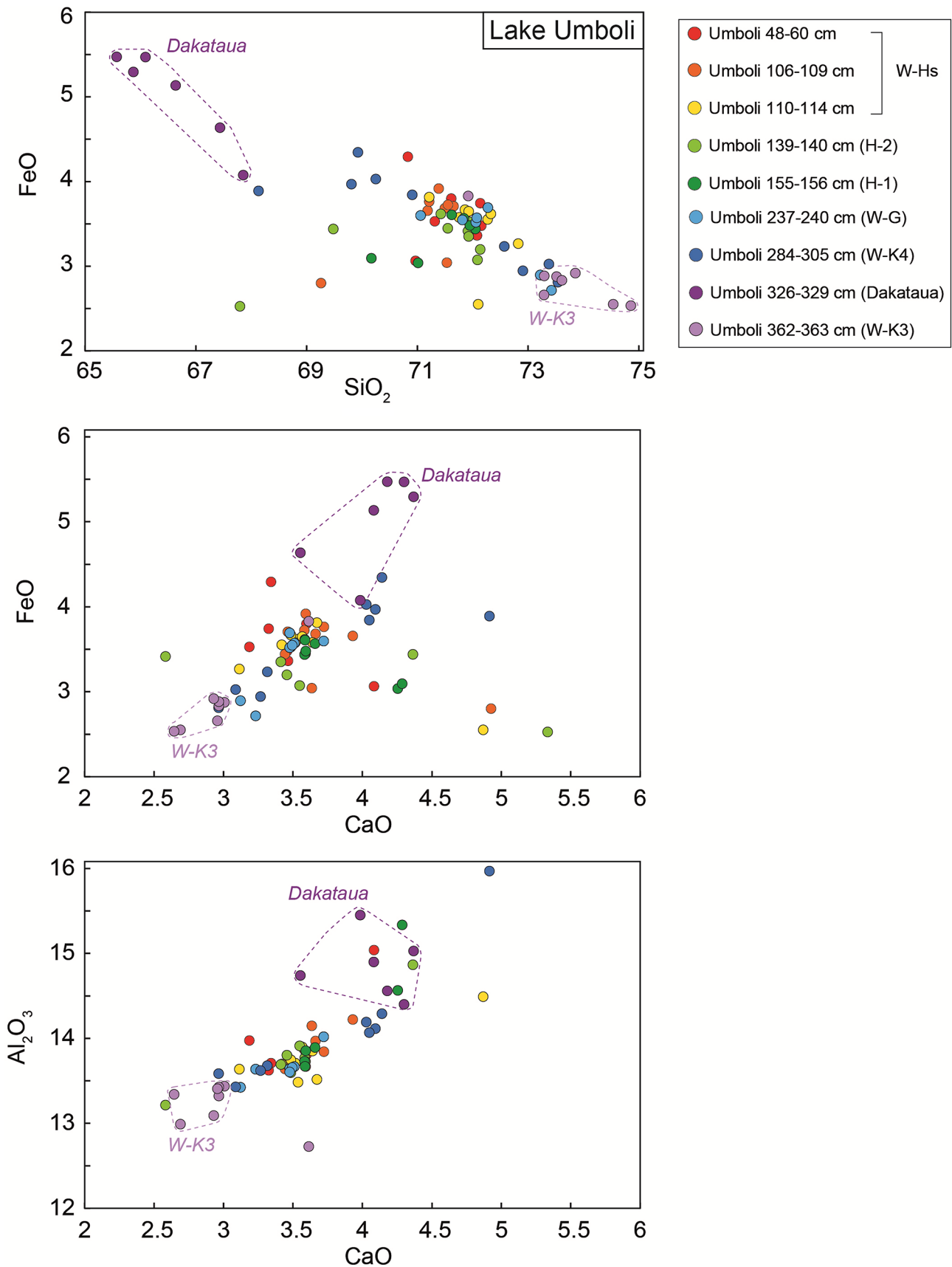


Figure 12. Volcanic glass chemistry for tephras obtained from Lake Umboli. Fields around the 362–363 cm and 326–329 cm samples correlate with W-K3 and Dakataua tephras, respectively (Fig. 11). Tephras labelled in the legend are deduced based on stratigraphic position, thickness, and radiocarbon dates; see discussion.

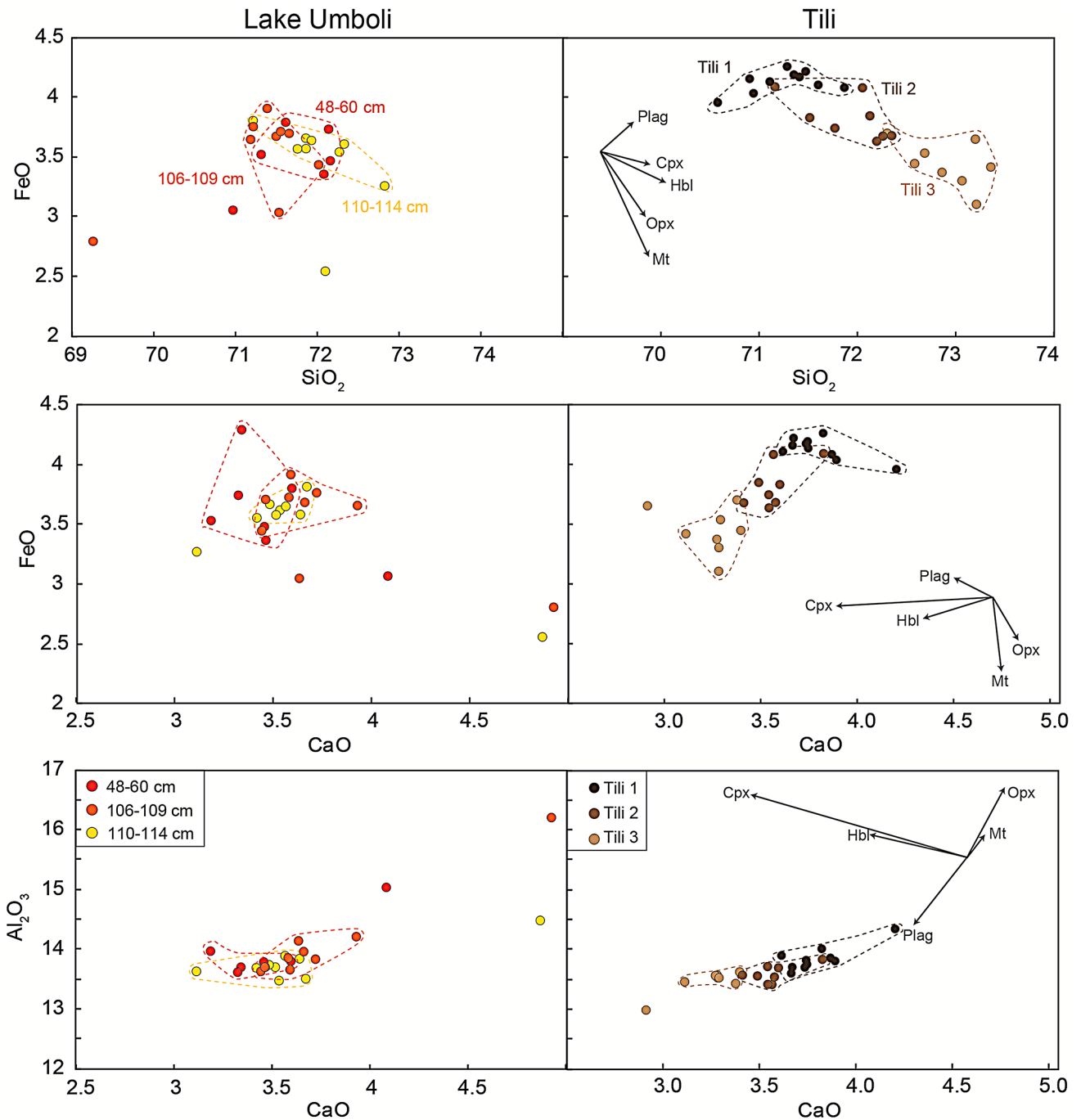


Figure 13. Volcanic glass compositions for the W-H eruptions at Lake Umboli are compared with the volcanic glass compositions at Tili. Mineral vectors are from Fig. 11; note that they are shrunk to fit in the space. Fields drawn around individual tephra samples do not include extreme outliers. The three Tili tephra samples are compositionally distinct, while Lake Umboli samples have considerable overlap.

H2 and superposition distinguish the Hoskins 1 (H1) and Hoskins 2 (H2) tephtras. Of particular note in this core is the identification of a very thin lamella of peat preserved within H2 indicating there was a short time interval between the deposition of the upper and lower beds.

The analyses of the three tephtras at the Tili site show a fit with the W-H tephtra group and a remarkably clear sequence of decreasing SiO_2 and increasing FeO, CaO and Al_2O_3 with time, with very little overlap (middle panel Fig. 13).

Tephtras from the Garu site are less straight-forward (Fig. 14), although Garu 1 and 2 have slightly higher FeO contents than Garu 3-4. Because they represent the uppermost two thin tephtras in the region it is highly likely that they are W-H6 and W-H7. The lowermost tephtra, Garu 5, lies stratigraphically between radiocarbon dates of 775 ± 35 BP (OZF 371) and

725 ± 60 BP (OZG 283) (Jago and Boyd, 2005). Hence this tephtra is older than the W-H tephtra series as reported by Machida *et al.* (1996) and must be a correlative of either Hoskins 1 or Hoskins 2. From the known record preserved in Lake Umboli, this tephtra is likely to be H2 due to its greater thickness. Hence, the two tephtras (3 samples) between are likely to represent the W-H4 and W-H5 tephtras, since W-H3 is of very restricted distribution (see fig. 5F in Machida *et al.*, 1996).

The results from Kulu 1 show correlation with the W-H tephtras (Fig. 14). Analyses from Kulu 2 show the top three samples have a similar identification, but Kulu 2/4, being post-W-K4, fits with a W-G identification, as does Kulu 3 (Fig. 15). The sample from Kulu 6 shows variation between the W-H field, and W-G/H2.

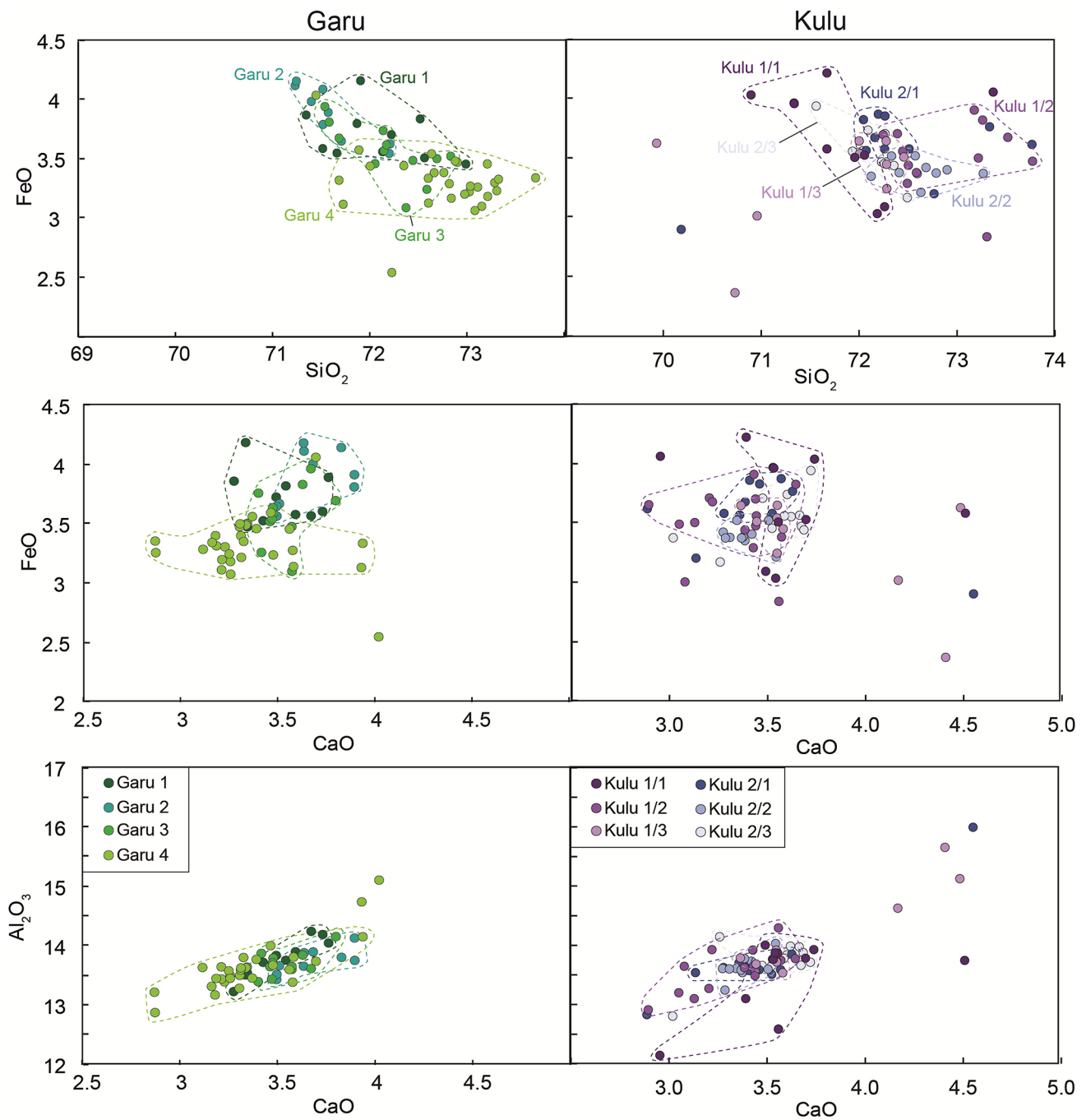


Figure 14. Volcanic glass compositions for the post-W-K4 eruptions from the Garu 1 and 2 sites, and Kulu 1 and Kulu 2 sites. Fields drawn around individual tephra samples do not include extreme outliers. All data overlap considerably, especially in CaO vs Al₂O₃, although Garu 1 and 2 samples extend to somewhat higher FeO.

Discussion Tephra correlation

The volcanic glass geochemistry of the four Holocene plinian eruptions from Witori caldera (W-K1 to W-K4) have been used to elucidate the identification of unproven tephra correlatives across the Willaumez isthmus region. In addition it has assisted in the identification of alluvial pumice which has been rapidly transported from the nearby mountains down the Kulu-Dulagi River to the lowlands, after the W-K2 eruption, infilling an embayment of the sea to create much of the land forming the Willaumez isthmus.

The volcanic glass geochemistry also allowed unequivocal identification of the lower three tephras in the Lake Umboli core, acting as a strong stratigraphic base line for identifying the overlying tephras (Fig. 2). Using geochemistry and radiocarbon dating of the peat intervals,

the next three tephras above are correlated with the W-G (Galilo Pumice of Blake, 1976), H1, and H2 tephras (Machida *et al.*, 1996) respectively. Of the tephras preserved between 40 and 114 cm depth in our core, it is clear that none of them match the youngest two thin (1 cm thick) tephras preserved at the Tili site, which show a higher FeO content (Fig. 13). Hence, we interpret that the uppermost tephras in our Lake Umboli core are highly likely to be W-H4 and W-H5 based on the coarseness and thickness of the samples together with the known radiocarbon dating. A thin (< 2 cm) tephra retrieved in a previous unpublished core from Lake Umboli apparently has W-H6 preserved above W-H5.

The three tephras at the Tili site (Fig. 3) are interpreted as W-H6, 5 and 4 (from surface down) based on their glass analyses, thickness and grain size (W-H3 and W-H7 being of more restricted distribution).

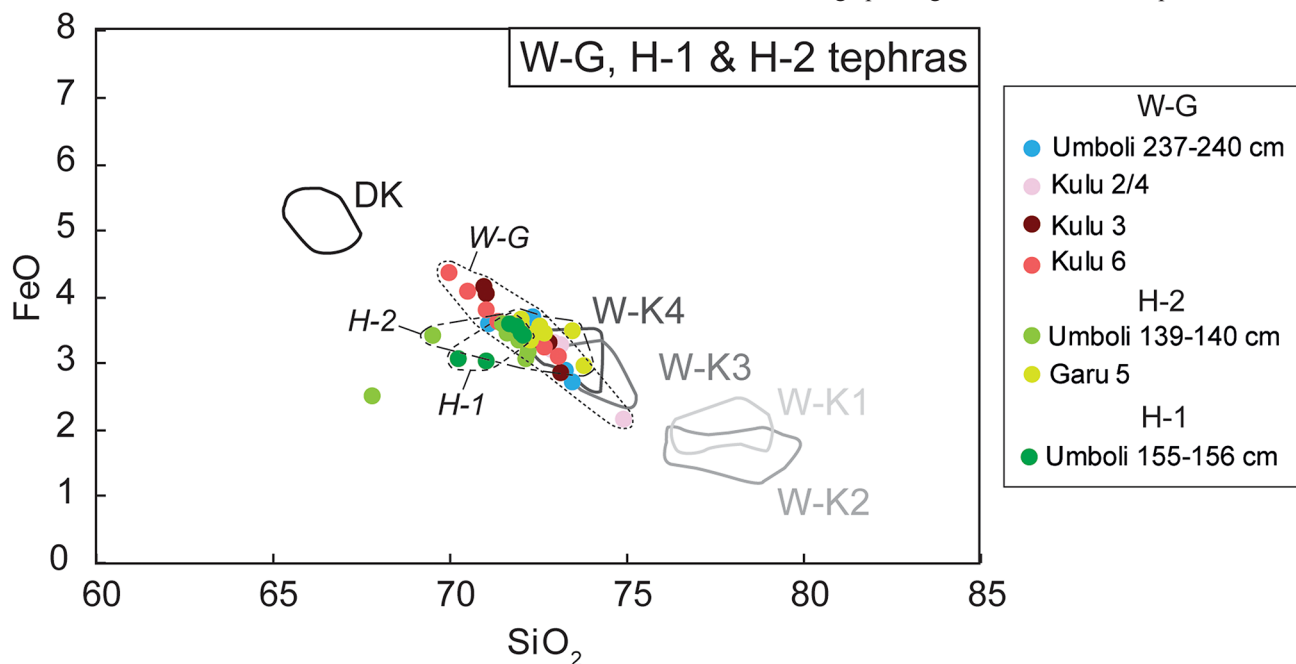


Figure 15. FeO vs SiO₂ for tephra samples from Umboli, Garu and several Kulu sites identified as post the W-K event but before the W-H tephras (based on their stratigraphic position, thickness and radiocarbon dates) show considerable compositional overlap, making correlations challenging based on microprobe data. Fields for Dakataua (DK) and W-K1 to 4 are from Fig. 11.

Glass analyses of the four uppermost tephras at the Garu site (Fig. 14) show they belong to the W-H group. The top two tephras are relatively thin and therefore are a likely match with W-H6 and H7; the lower two correlate with W-H5 and H4. The lowermost tephra (Garu 5) is in a similar stratigraphic position and with similar geochemistry to match with a Hoskins tephra, either H1 or H2. Based on the relative thicknesses of these two tephras in the Lake Umboli core, this tephra is highly likely to be H2.

The three Kulu 1 samples (Fig. 14) are clearly W-H tephras, and are here correlated to W-H6, 5 and 4. The uppermost, W-H6 has probably been overthickened by slight colluvial redeposition.

At Kulu 2 (Fig. 6) there are four samples analysed in stratigraphic order above W-K4. All show overlapping geochemistry which does not enable unequivocal identification (Fig. 14). Based on its stratigraphic position (i.e., post-W-K4) and its geochemistry, sample Kulu 2/4 here correlates with W-G (Galilo Pumice) (Fig. 15). The tephras above are consistent with the geochemistry of the W-H and H tephras and their stratigraphic positions and thicknesses are here interpreted to represent the W-H5 (Kulu 2/1), W-H4 (Kulu 2/2) and H2 (Kulu 2/3) tephras.

The unknown sample from Kulu 3 (Fig. 7) is clearly a post-W-K4 tephra. Its stratigraphic position and geochemistry fit with it being W-G (Galilo Pumice) (Fig. 15).

The Kulu 4 sample is identified in the W-K1 or W-K2 group of geochemical analyses (Fig. 11). It is almost certainly W-K2 because it is the next primary pumiceous tephra beneath 1.22 m of redeposited W-K2 (Fig. 8). Of significance at this site is 10 cm of grey mud between the primary tephra and the redeposited pumice sand and gravel. This records a brief time interval between the deposition of the tephra and its fluvial redeposition from the headwaters of the Kulu-Dulagi River on to the coastal lowlands.

Kulu 5 analyses plot into the W-K2 geochemical field (Fig. 11). This tephra is found beneath W-K3 and beneath 1.5 m of redeposited pumiceous sand and silt (Fig. 9). In this case a 5 cm layer of pinkish light grey silt with organic staining separates the primary from the secondary redeposited W-K2

pumice, recording a brief hiatus.

The unknown sample from Kulu 6 (Fig. 10) shows a spread of geochemical analyses that are equivocal (Fig. 15). Based on its post-W-K4 stratigraphic position and depth below the obvious W-H tephras, it is here correlated to Galilo Pumice (W-G).

Correlation columns of all sites are plotted in Fig. 16, from north-west to south-east and then north to FAAH.

The Garu, Kulu 1 and Kulu 4 records represent the current swampy lowland environment of deposition; the Tili site is a levee alongside a former loop of the Kulu-Dulagi River. The Kulu 3, 5 and 6 sites are all on well drained mounds within the lowlands preserving mostly tephras rather than alluvial deposits. In contrast the Kulu 2 site is an exposure on a hill bordering the southern limits of the Kulu lowlands and hence is well drained and preserves a tephra accretion sequence without interbedded sediments. FAAH is a plateau-topped hill near the eastern coast which is well drained and entirely comprised of tephras. From a paleoenvironmental perspective, it is the Lake Umboli core which is most unusual. Apart from the top 40 cm of unconsolidated lake mud, the remaining time intervals between the identified tephras are represented by black fibrous peat and not lacustrine sediments. This implies one of two scenarios. Either Lake Umboli has risen suddenly over the last 400 years by > 10 m, or it has been gradually rising over the last 1800 years and the peat in the core accumulated marginal to a rising lake level.

The unexpected rubble deposit within the core between 170 and 218 cm depth (Fig. 2) is most likely the result of a natural erosion event on the inner wall of the Lake Umboli depression. This could be either due to (a) a storm-induced erosion event that might be related to a rare tropical cyclone in this region or (b) to a large regional or local shallow earthquake triggering collapse of the Lake Umboli depression's inner wall and accompanying or subsequent heavy rain. The deposit appears to be of a similar age to a tsunami deposit identified on Boduna Island, 40 km to the north off the east coast of the Peninsula (White *et al.*, 2002), suggestive of a large magnitude regional earthquake at this time.

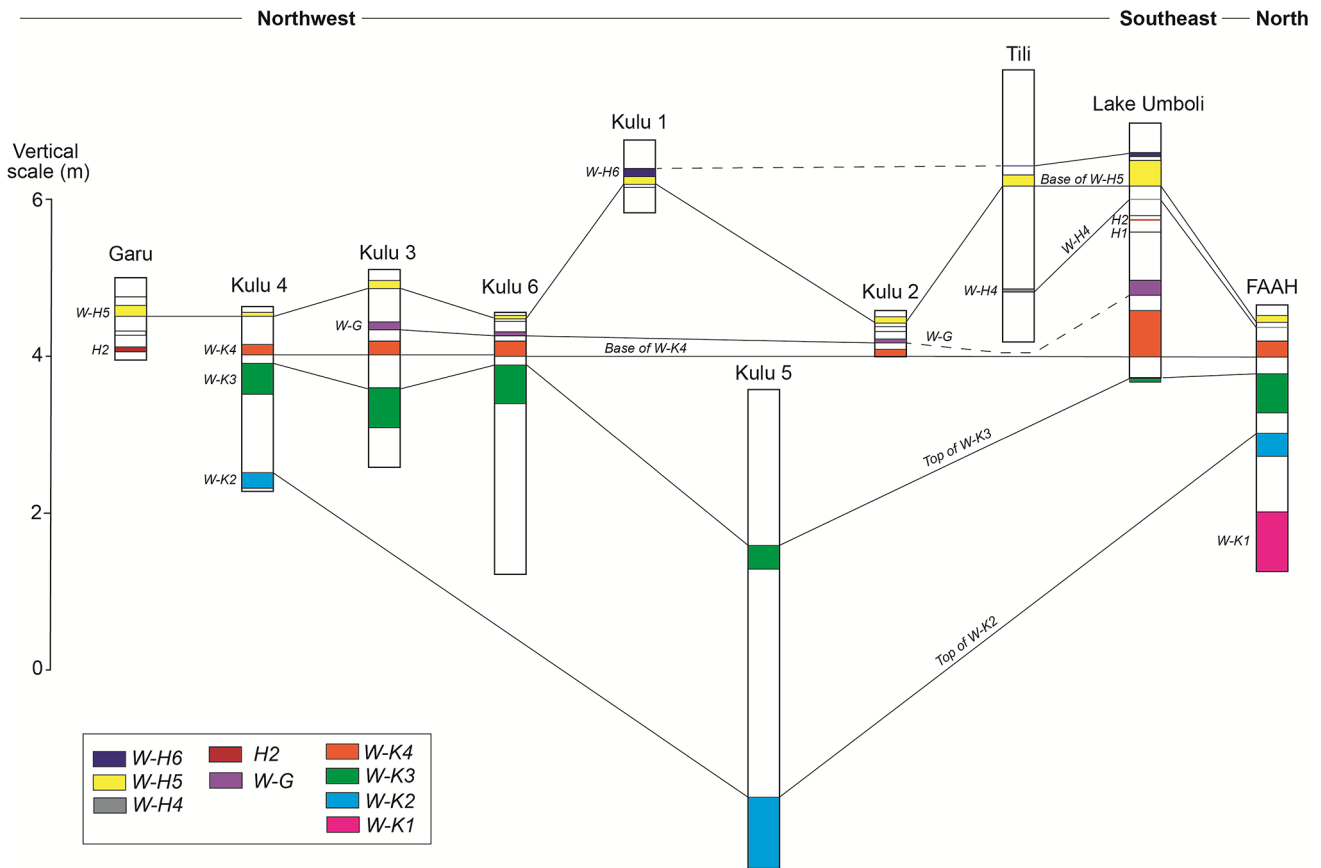


Figure 16. Correlation of stratigraphic columns showing summary tephra identifications between sites described in this paper.

Petrogenesis

All data in this study lie along a similar trend in the chemical plots presented in Figs 11, 12 and 15. Such trends could suggest that the magmas involved are broadly related by fractional crystallisation of genetically similar magmas. Fractional crystallisation vectors shown in Figs 11 and 13 use compositions of phases known to be present in the lavas and tephtras of the Witori caldera (Machida *et al.*, 1996): see Fig. 11 caption and Table S1 for mineral compositions used in calculating vectors. Glass chemistry is an effective means of assessing melt evolution changes as the shards represent the evolving melt composition without dilution by the phenocrysts. As mineral chemistry is not available for the Witori or Dakataua eruptions, compositions are used from Tauhara volcano in the Taupo Volcanic Zone of New Zealand (Millet *et al.*, 2014), as this is a continental arc dacite with a similar mineral assemblage. The W-K3/4 tephtras are less evolved than the preceding W-K1/2 tephtras; this can be explained by approximately 15% crystallisation of a combination of plagioclase, clinopyroxene, hornblende and magnetite (0.47 : 0.25 : 0.25 : 0.03) between W-K3/4 and W-K1/2-like magma compositions.

This suggests that although the Witori eruptions had the

same magmatic source, separate magmatic reservoirs with their own magma histories and timescales may have fuelled the individual eruptions. Similar major element compositions with increasing SiO₂ content for the W-K1 and W-K2 group tephtras suggest that the magmas were not strongly affected by fractional crystallisation once attaining high SiO₂ contents; the difference in FeO between W-K1 and W-K2 may be due to small amounts of magnetite crystallisation between magma batches. Although the W-K3 and W-K4 tephtras overlap in composition, negative and positive trends in FeO and Al₂O₃ (respectively) with SiO₂ are suggestive of a greater control by fractional crystallisation within these magmas than in the higher SiO₂ tephtras. In the Tili samples there is a small gradual change in magma composition most likely due to crystallisation of the mineral assemblage mentioned above between each tephtra-producing eruption. Dakataua compositions have comparatively higher FeO and Al₂O₃ than the W-K trend which indicates a somewhat different petrogenetic evolution, as may be expected since they originate from a volcanic system approximately 50 km north of Witori caldera. Further interpretations of the magma generation in these large systems would require a more detailed petrographic and geochemical study involving isotopic data and mineral chemistry.

Conclusion

This study demonstrates the usefulness of volcanic glass geochemistry to enhance stratigraphic and tephra granulometry information for correlating tephtras at distal locations, in this case in Papua New Guinea. This work recognises that individual tephtras cannot currently be distinguished on unique geochemical criteria but combined with known stratigraphic position can lead to specific identification. The geochemistry is sufficient to distinguish tephra subgroupings that probably match phases of fractional crystallisation of the parent magmas. This has helped strengthen tephra identification and correlation on the Willaumez isthmus which ultimately assists in better constraining the age of Holocene archaeological sites in the region. Future work should involve analysis of Holocene tephtras by laser ablation inductively coupled plasma mass spectrometry (LA-ICP-MS) to obtain high precision trace element data for individual stratigraphic units. This technique has been effectively used in other tephrochronological studies to fingerprint tephtras from a small, highly active region of small scale eruptions (the Quaternary Auckland Volcanic Field: Hopkins *et al.*, 2015) and also applied to archaeological sites on the Sepik coast of Papua New Guinea (Golitzko *et al.*, 2010).

Supplementary data

<https://doi.org/10.6084/m9.figshare.14502618>

Table S1. Supplementary data is published separately at *figshare*.

Raw and normalised volcanic glass data and standards. All raw and normalised glass chemistry data for the Dakataua tephra, FAAH site and Kulu, Garu and Tili plantation sites are presented in order of depth. Mineral standard data for the analytical sessions and literature data for the fractional crystallisation vectors in Figs 11 and 13 are also given in Neall (2021).

Analytical totals for glass are < 100% due to post-eruption hydration (Shane, 2000), for consistency all major element data presented in figures are normalised to 100%. Both raw and normalised data are presented in Neall (2021).

ACKNOWLEDGMENTS. This work would not have been accomplished but for the leadership of Robin Torrence. To her we owe a great debt of gratitude. Sincere appreciation is also expressed to Lucy Pearse who assisted in the laboratory separation of volcanic glass and to Bill Boyd who accompanied VN in discovering and sampling three of the Kulu sites and the Tili site. We also gratefully thank R. B. Stewart, F. L. Sutherland and an anonymous reviewer for their helpful comments on this paper.

References

- Blake, D. 1976. Pumiceous pyroclastic deposits of Witori volcano, New Britain, Papua New Guinea. In *Volcanism in Australia*, ed. R. W. Johnson, pp. 191–200. Amsterdam: Elsevier.
- Golitzko, M., J. Meierhoff, and J. E. Terrell. 2010. Chemical characterization of sources of obsidian from the Sepik coast (PNG). *Archaeology in Oceania* 45(3): 120–129. <https://doi.org/10.1002/j.1834-4453.2010.tb00088.x>
- Hopkins, J. L., M.-A. Millet, C. Timm, C. J. Wilson, G. S. Leonard, J. M. Palin, and H. Neil. 2015. Tools and techniques for developing tephra stratigraphies in lake cores: a case study from the basaltic Auckland Volcanic Field, New Zealand. *Quaternary Science Reviews* 123: 58–75. <https://doi.org/10.1016/j.quascirev.2015.06.014>
- Jago, L. C. F., and W. E. Boyd. 2005. How a wet tropical rainforest copes with repeated volcanic destruction. *Quaternary Research* 64: 399–406. <https://doi.org/10.1016/j.yqres.2005.08.012>
- Lowe, D. J., N. J. G. Pearce, M. A. Jorgensen, S. C. Kuehn, C. A. Tryon, and C. L. Hayward. 2017. Correlating tephtras and cryptotephtras using glass compositional analyses and numerical and statistical methods: review and evaluation. *Quaternary Science Reviews* 175: 1–44. <https://doi.org/10.1016/j.quascirev.2017.08.003>
- Machida, H., R. J. Blong, H. Moriwaki, J. Specht, R. Torrence, Y. Hayakawa, B. Talai, D. Lolo, and C. F. Pain. 1996. Holocene explosive eruptions of Witori and Dakataua caldera volcanoes in West New Britain, Papua New Guinea. *Quaternary Research* 34–36: 65–78. [https://doi.org/10.1016/1040-6182\(95\)00070-4](https://doi.org/10.1016/1040-6182(95)00070-4)
- McKee, C. O., V. E. Neall, and R. Torrence. 2011. A remarkable pulse of large-scale volcanism on New Britain Island, Papua New Guinea. *Bulletin of Volcanology* 73: 27–37. <https://doi.org/10.1007/s00445-010-0401-8>
- Millet, M.-A., C. M. Tutt, M. R. Handler, and J. A. Baker. 2014. Processes and time scales of dacite magma assembly and eruption at Tauhara volcano, Taupo Volcanic Zone, New Zealand. *Geochemistry, Geophysics, Geosystems* 15(1): 213–237. <https://doi.org/10.1002/2013GC005016>
- Neall, V. 2021. [Supplementary data. Raw and normalised volcanic glass data and standards—Willaumez isthmus]. *figshare*. Dataset. <https://doi.org/10.6084/m9.figshare.14502618>
- Neall, V. E., R. C. Wallace, and R. Torrence. 2008. The volcanic environment for 40,000 years of human occupation on the Willaumez Isthmus, West New Britain, Papua New Guinea. *Journal of Volcanology and Geothermal Research* 176(3): 330–343. <https://doi.org/10.1016/j.jvolgeores.2008.01.037>
- Petrie, C. A., and R. Torrence. 2008. Assessing the effects of volcanic disasters on human settlement in the Willaumez Peninsula, Papua New Guinea: a Bayesian approach to radiocarbon calibration. *The Holocene* 18(5): 729–744. <https://doi.org/10.1177/0959683608091793>
- Potts, P. J., M. Thompson, S. Wilson, and P. Webb. 2005. G-probe-2—an international proficiency test for microbeam laboratories—report on round 2/May 2005 (NKT-1G basaltic glass). *Geostandards Newsletter*.
- Shane, P. 2000. Tephrochronology: a New Zealand case study. *Earth-Science Reviews* 49(1): 223–259. [https://doi.org/10.1016/S0012-8252\(99\)00058-6](https://doi.org/10.1016/S0012-8252(99)00058-6)

- Specht, J., and R. Torrence. 2007. Lapita all over: land-use on the Willaumez Peninsula, Papua New Guinea. In *Oceanic Explorations: Lapita and Western Pacific Settlement*, ed. S. Bedford, C. Sand, and S. P. Connaughton, pp. 71–96. Terra Australis 26. Canberra: ANU E Press.
<https://doi.org/10.22459/TA26.2007.04>
- Torrence, R., V. Neall, and W. E. Boyd. 2009. Volcanism and historical ecology on the Willaumez Peninsula, Papua New Guinea. *Pacific Science* 63(4): 507–535.
<https://doi.org/10.2984/049.063.0404>
- Torrence, R., V. Neall, T. Doelman, E. Rhodes, C. McKee, H. Davies, R. Bonetti, A. Guglielmetti, A. Manzoni, M. Oddone, J. Parr, and C. Wallace. 2004. Pleistocene colonisation of the Bismarck Archipelago: a different pattern in West New Britain? *Archaeology in Oceania* 39(3): 101–130.
<https://doi.org/10.1002/j.1834-4453.2004.tb00568.x>
- Torrence, R., J. Specht, and R. Fullagar. 1990. Pompeiis in the Pacific. *Australian Natural History* 23(6): 456–463.
- White, J. P., C. Coroneos, V. E. Neall, W. Boyd, and R. Torrence. 2002. FEA site, Boduna Island: further investigations. In *Fifty Years in the Field. Essays in Honour and Celebration of Richard Shutter Jr's Archaeological Career*, ed. S. Bedford, C. Sand, and D. Burley, pp. 101–107. New Zealand Archaeological Association Monograph 25. Auckland: New Zeal Archaeological Association.